Measurement of the pp $\rightarrow$ WZ inclusive and differential cross-sections, polarization angles and search for anomalous gauge couplings at $\sqrt{s} = 13$ TeV

CMS PAS SMP-20-041, CMS Collaboration

Ricardo Barrué

SFRH/BD/150792/2020

Outline

Outline

Introduction

Studied $pp \to WZ$ production in the $\ell\bar{\ell}\,\ell'$ final state, $\mathcal{L} = 137\ \mathrm{fb}^{-1}$.

- large cross-section and high purity
- sensitive to the parton distribution function (PDF) of the *u* and *d* quarks and to triple gauge couplings (TGC)
- dominant background in BSM searches with similar final states (e.g. arXiv:2106.01676)

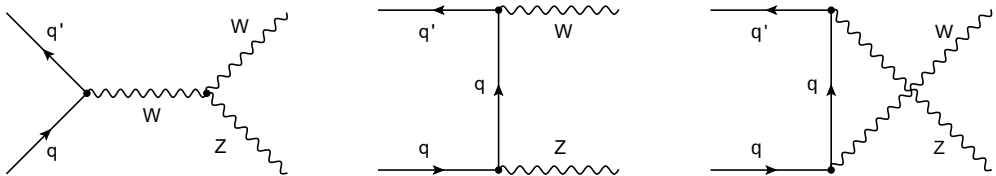

Figure 1: Tree-level Feynman diagrams of *WZ* production.

Outline

The CMS detector

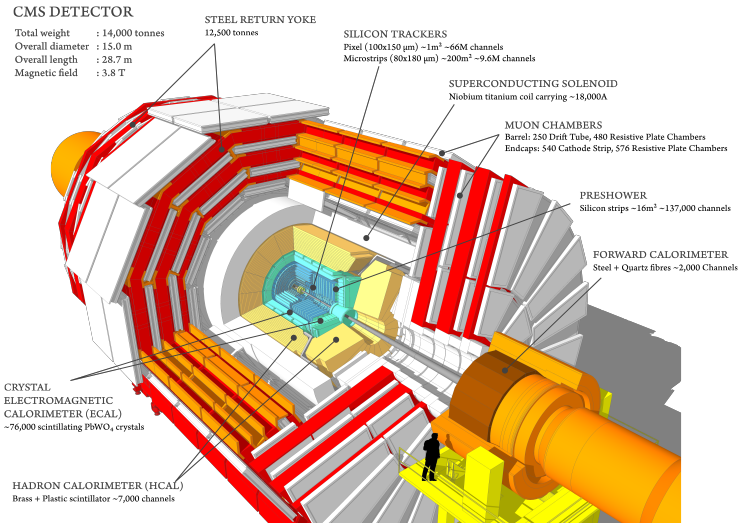

Outline

Dominant backgrounds

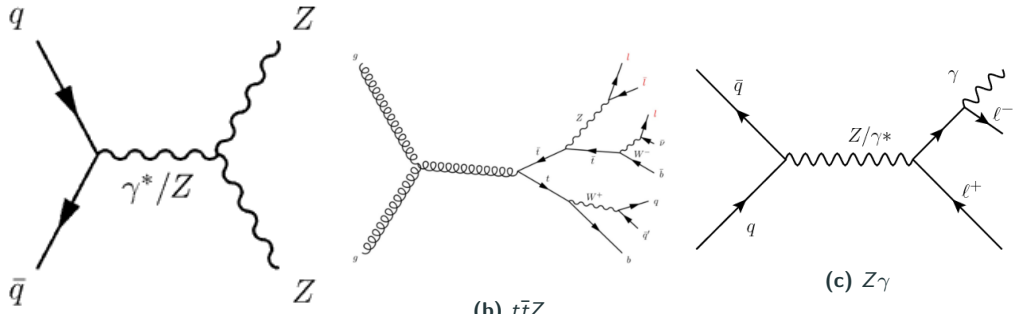

(a) ZZ **(b)** $t\bar{t}Z$ **(c)** $Z\gamma$

Figure 2: Example Feynman diagrams of the dominant background processes

Event reconstruction and object selection

Electrons: charged particle in the tracking system + matching energy depositions in the ECAL and photons along the trajectory

- $p_T > 7$ GeV and $|\eta| < 2.5$

Muons: combination of tracks from the silicon trackers and muon chambers

- $p_T > 5$ GeV and $|\eta| < 2.4$

Isolation and MVA-based identification criteria applied on the leptons (*tight* leptons)

- isolate *prompt* from *nonprompt* contributions

Missing transverse momentum (p_T^{miss}): negative vector-sum of the p_T of all PF objects selected in the event

Triggers and signal region (SR) event selection

Events are selected in real-time by single- and double-lepton triggers.

To obtain a high purity signal region (SR), several cuts are applied:

1. three *tight* light leptons
2. ≥ 1 opposite-sign same-flavour lepton pair
3. $p_T(\ell_{Z1}) > 25$ GeV, $p_T(\ell_{Z2}) > 10$ GeV, $p_T(\ell_W) > 25$ GeV
4. $|M(\ell_{Z1}, \ell_{Z2}) - M_Z| < 15$ GeV
5. $p_T^{\text{miss}} > 30$ GeV
6. $M(\ell_{Z1}, \ell_{Z2}, \ell_W) > 100$ GeV
7. veto events with at least one *b*-tagged jet
8. veto events with a fourth lepton passing looser ID criteria
9. min $M(\ell, \ell') > 4$ GeV

Events separated into flavour-composition channels: *eee*, $ee\mu$, $\mu\mu e$ and $\mu\mu\mu$.

Background control regions (CR)

Background control regions (CR) are defined.

- dominated by one of the relevant backgrounds, used to estimate its normalization

ZZ CR:

- require a fourth *tight* lepton, $p_T(\ell) > 10$ GeV
- $p_T^{\text{miss}} < 30$ GeV

$t\bar{t}Z$ CR ($t\bar{t}Z$, $t\bar{t}W$, tZq): inverting the b-tagged jet veto

Conversion CR:

- remove the $|M(\ell_{Z1}, \ell_{Z2}) - M_Z|$ cut
- $M(\ell_{Z1}, \ell_{Z2}, \ell_W) < 100$ GeV

Post-fit distributions I

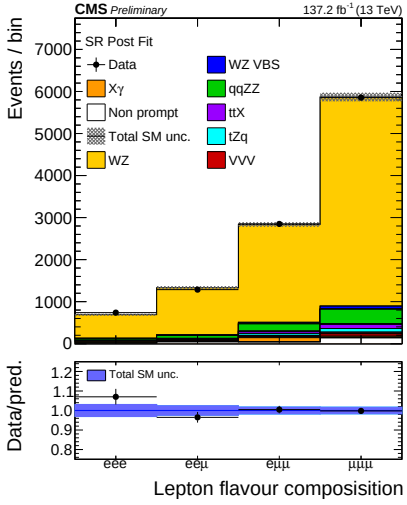

(a) SR

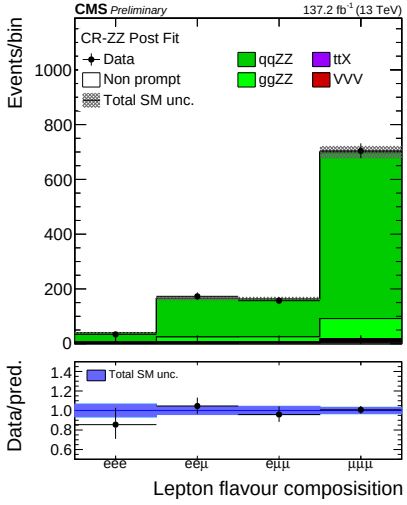

(b) ZZ CR

Post-fit distributions II

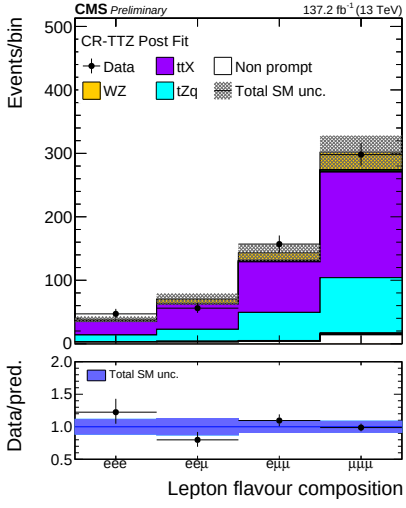

(a) $t\bar{t}Z$ CR

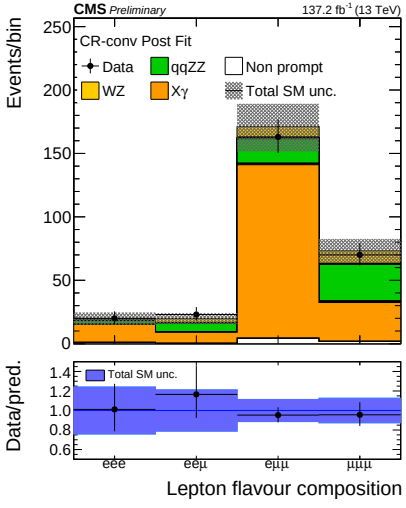

(b) $Z\gamma$ CR

Outline

Cross-section measurement

Yields in WZ SR obtained by a maximum-likelihood fit to yields in the SR and CR.

- measurement performed in the flavour-inclusive and flavour-exclusive categories

Results are extrapolated to a fiducial region (FR), by calculating the ratio between SR and FR efficiencies, ϵ.

$$\sigma_{fid}(pp \to WZ) = \frac{N_{WZ}^{SR}}{\epsilon \mathcal{L}} \left(\frac{N_{fid}^{SR}}{N_{tot}^{SR}} \right) \tag{1}$$

Results are extrapolated to a total region (TR), by calculating the acceptance factor from the total to the fiducial region, $\mathcal{A}$.

$$\sigma_{tot}(pp \to WZ) = \frac{N_{WZ}^{SR}}{BR(W \to \ell\nu) BR(Z \to \ell'\ell') \mathcal{A} \epsilon \mathcal{L}} \left(\frac{N_{fid}^{SR}}{N_{tot}^{SR}} \right) \tag{2}$$

Total cross-section measurement results

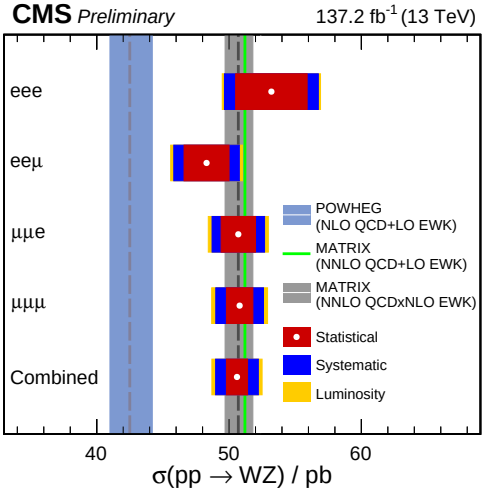

Results in agreement with SM predictions

- favour fixed-order calculations from MATRIX at NNLO QCD with multiplicative combination of NLO EW corrections

Outline

Charge asymmetry measurement

Charge asymmetry in WZ production allows access to the u and d quark PDFs.

$$A^{+-}(WZ) = \frac{\sigma_{fid}(pp \to W^+Z)}{\sigma_{fid}(pp \to W^-Z)} \tag{3}$$

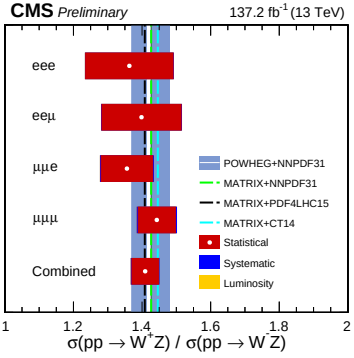

Asymmetry measurement:

- in agreement with NLO and NNLO predictions, similar agreement between both
- strong consistency with the `NNPDF30_nlo_as118` PDF set

Used to reduce PDF uncertainties in the cross-section measurements.

Outline

Introduction and methodology

Possible new physics in the WZ production vertex can affect boson spin observables.

In this work, the W (Z) polarization angle θ^W (θ^Z) is defined in the helicity frame:

- the angular distance between the momenta of the child lepton (negatively charged lepton) in the rest frame of the W (Z) boson and the momenta of the W (Z) boson in the lab frame

One can write the differential cross-sections as a function of $\cos\theta^{W\pm}$ and $\cos\theta^Z$

- depend on the polarization fractions, $f_{L,R,0}^{W,Z}$.

Maximum-likelihood fit to the $\cos\theta^{W\pm}$ and $\cos\theta^Z$ distributions in the charge-inclusive and the two different final state charge regions.

Results

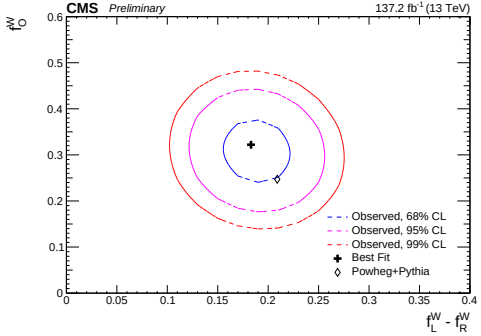

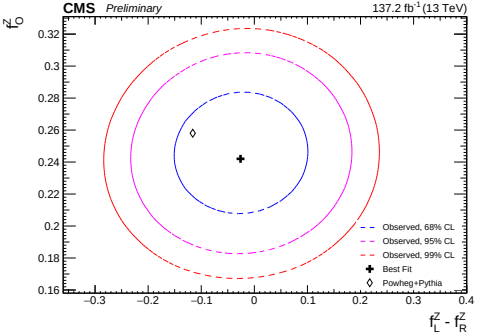

Results behave according to SM predictions.

- first observation of longitudinally polarized W bosons ($f_0^W \neq 0$) in the WZ channel

Outline

Introduction and methodology

Differential WZ cross-sections measured in the total production phase space as a function of several observables:

- energy scale of WZ production: p_T^Z, p_T^W, $p_T^{\text{lead jet}}$, $N_{textjet}$
- $\cos\theta^{W\pm}$ and $\cos\theta^Z$
- $M(WZ)$

Generator-level distributions are obtained by *unfolding* of the reconstruction-level distributions.

- derive *response* matrices - model the migrations between generator-level and reconstructed-level bins

Results

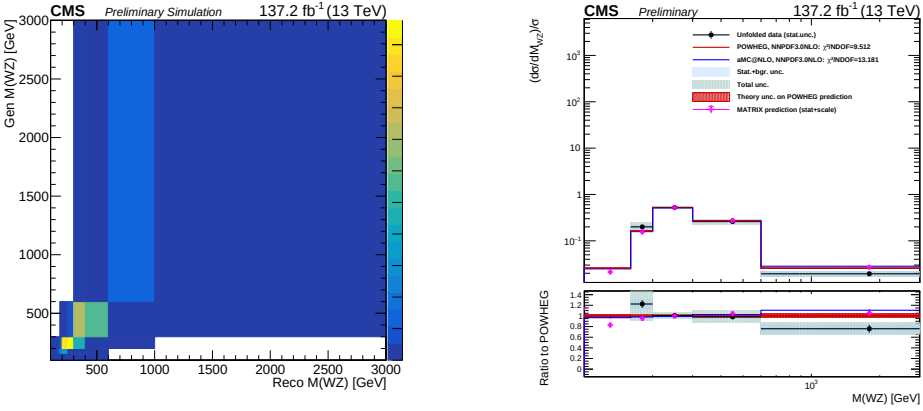

Figure 6: Response matrix (left) and differential cross-section (right) for the $M(WZ)$ observable

Differential cross-section results for this variable are mostly compatible with the SM.

Outline

Introduction and methodology

WZ process is sensitive to anomalous TGCs in the *WWZ* vertex

- may come from BSM physics directly observable only at higher energies
- can be parametrized by adding dimension-6 operators to the SM *WWZ* Lagrangian

Taking into account 3 CP-conserving and 2 CP-violating dimension-6 operators.

A 3D (2D) quadratic fit to the $M(WZ)$ distribution is done in a grid of multiple values of the Wilson coefficients of the CP-conserving (CP-violating) operators.

- possible correlations between the CP-conserving terms are studied

Results

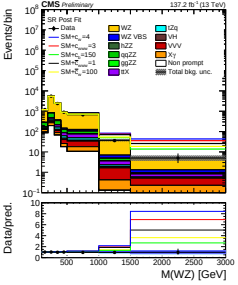

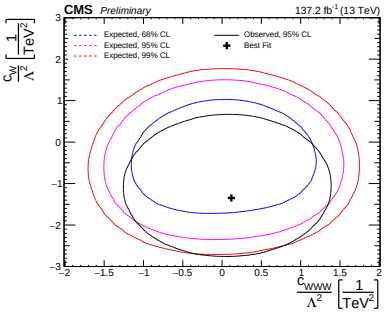

Parameter	95% CI, Exp. (TeV^{-2})	95% CI, Obs. (TeV^{-2})	Best fit, Obs. (TeV^{-2})
c_W/Λ^2	$[-2.05, 1.27]$	$[-2.52, 0.33]$	-1.34
c_{WWW}/Λ^2	$[-1.27, 1.33]$	$[-1.04, 1.19]$	0.15
c_b/Λ^2	$[-86.0, 125.0]$	$[-42.7, 113.0]$	43.6
$\tilde{c}_{WWW}/\Lambda^2$	$[-0.76, 0.65]$	$[-0.62, 0.53]$	-0.03
$\tilde{c}_W/\Lambda^2$	$[-46.1, 46.1]$	$[-45.9, 45.9]$	0.0

Results are **within the SM expectations**.

Outline

Data and simulated samples

Dataset used: *pp* collisions, $\mathcal{L} = 137\ \mathrm{fb}^{-1}$ (full LHC Run 2)

MC event generators:

- nominal signal: `POWHEG-box` at NLO in QCD
- alternative signal: `Madgraph5_aMC@NLO` at NLO in QCD
- backgrounds: `POWHEG` and `Madgraph5_aMC@NLO` at NLO in QCD

Simulated events are interfaced with Pythia8 and Geant4 detector simulation.

`MATRIX` for cross-section calculations at NNLO in QCD

- possible inclusion of NLO EW corrections

Event reconstruction and object selection

Vertices: grouping tracks consistent with originating from the same location in the beam interaction region

- primary collision vertex chosen as the one with largest value of $\sum p_T^2$ of associated jets

Jets: anti-k_t clustering algorithm to the PF candidates

- $p_T > 25$ GeV, $|\eta| < 2.5$
- $\Delta R(\ell, j) < 0.4$
- b-jets are tagged using the DeepCSV algorithm

Trigger selection

- single-lepton: 27-35 (24-27) GeV for electrons (muons)
- double-muon: 17 (8) GeV for the leading (subleading) muon
- double-electron: 23 (12) GeV for the leading (subleading) electron
- electron-muon: 23 (8 or 12) GeV for the leading lepton (subleading muon or electron)

Systematic uncertainties

Source	2016	2017	2018	Correlation scheme	Processes
Electron efficiency	$0-3.3$	$0-3.0$	$0-2.8$	Partially correlated	All MC
Muon efficiency	$0-2.4$	$0-2.1$	$0-2.0$	Partially correlated	All MC
Muon energy scale	$0-5$	$0-5$	$0-5$	Correlated	All MC
Electron energy scale	$0-5$	$0-5$	$0-5$	Correlated	All MC
Trigger efficiency	$-1.0/0.6$	$-0.7/0.6$	$-0.7/0.6$	Partially correlated	All MC
Jet energy scale	0.9	0.7	1.1	Partially correlated	All MC
B-tagging (heavy)	1.0	0.7	0.9	Correlated	All MC
B-tagging (light)	0.5	0.4	0.3	Correlated	All MC
Pileup	0.9	0.8	0.8	Correlated	ALL MC
ISR	$0.2-20$	$0.2-20$	$0.2-20$	Correlated	WZ
Nonprompt norm.	30	30	30	Correlated	nonprompt
VVV norm.	50	50	50	Correlated	VVV
VH norm.	25	25	25	Correlated	VH
WZ VBS norm.	20	20	20	Correlated	WZ VBS
ZZ	Free	Free	Free	Correlated	ZZ
$t\bar{t}Z$ norm.	Free	Free	Free	Correlated	$t\bar{t}X$
tZq norm.	Free	Free	Free	Correlated	tZq
$X\gamma$ norm.	Free	Free	Free	Correlated	$X\gamma$
Luminosity	2.5	2.3	2.5	Partially correlated	All MC
Statistical uncertainties	By bin	By bin	By bin	Decorrelated	All MC
Theoretical (PDF + Scale)	0.9	0.9	0.9	Correlated	WZ

Figure 8: Summary of uncertainties in the analysis